QUBIC
IN2P3 Scientific Council

July 3rd, 2023

Abstract:

The quest for B-mode polarization of the Cosmic Microwave Background (CMB) is among the major challenges of observational cosmology. It would reveal primordial gravitational waves, validating inflation theory, with consequences in particle physics. The expected signal is weak, requiring high-sensitivity detectors.

QUBIC is an instrument based on Bolometric Interferometry, a new concept combining high sensitivity from bolometers and powerful systematics control from interferometry. QUBIC has the unique feature of spectral imaging. Foregrounds can be better mitigated by measuring their spectral properties within the physical band of the instrument.

After laboratory testing of the Technological Demonstrator (TD), identical to the "Full Instrument" but with fewer detectors and baselines, French/Italian agencies reviewed and validated its performance. The instrument was shipped to Argentina in 2021 and inaugurated at its 5000m a.s.l. site in November 2022 where commissioning is under progress.

A first upgrade will complete the "Full Instrument" only requiring procurement and integration of subsystems which have already been validated. As a conservative estimate, QUBIC will achieve $\sigma(r)=0.015$ after 3 years ($\sigma(r)=0.007$ including Planck and full covariance) in line with other competitors on similar timescales.
QUBIC is the only European-led B-mode project. It provides open-data, and has a rich education and outreach program.

Table of Contents

QUBIC: science case, concept and instrument status....2
Primordial Universe, inflation, and CMB Polarization....2
Detecting the CMB B-mode polarization: a considerable observational challenge....3
Bolometric Interferometry and QUBIC....5
Sensitivity:....5
Instrumental Systematics:....5
Spectral Imaging and astrophysical foregrounds:....6
QUBIC site:....7
QUBIC Status:....7
QUBIC timeline....10
Phase 1: On-sky demonstration of BI and Spectral Imaging with the QUBIC TD....10
Phase 2: QUBIC FI Science - Measurement of B-mode polarization down to $\sigma(r)=0.015$ (conservative)....11
New possibilities from Spectral Imaging with QUBIC....13
Ultra-Wide-Band instrument....13
Component Map-making....13
Detecting Dust Decorrelation with Spectral Imaging....14
Atmospheric mapping with spectral Imaging....15
Perspectives: Bolometric Interferometry beyond QUBIC....16

QUBIC: science case, concept and instrument status

Primordial Universe, inflation, and CMB Polarization

Our understanding of the Universe has significantly progressed over recent decades, mostly thanks to technological breakthroughs that have allowed for massive high-quality data to be compared to theoretical models, exhibiting impressive consistency [1]. While this led to the establishment of the *standard cosmological model* with a precise measurement of cosmological parameters, a number of tantalizing questions have appeared, such as the origin of the apparent acceleration of expansion [2, 3], or remain, such as the nature of Dark Matter [4] or what happened in the very early Universe [10, 5].

The search for primordial B-modes is related to the latter question: What is the physics of the early Universe? How was matter created in the first place? Why is the spatial curvature of the Universe so close to zero? Why are the observed inhomogeneities as small as 10^{-5}? What caused the primordial fluctuations which gave rise to the observed large-scale structure? The inflation paradigm [6, 7, 8, 9] proposes a solution to all of these questions through a period of accelerated expansion in the first fraction of a second (~10^{-35}s) after the Planck era [10]. Inflation is triggered by a scalar field, called inflaton, dominant in the energy budget of the Universe. During inflation, as the field potential slowly decreases, the Universe expands exponentially, tending to become flat and homogeneous. Inflaton quantum fluctuations are then transformed into macroscopic perturbation of the metric whose scalar and tensor modes do not decay with time [11]. This offers a physical mechanism for the initial conditions (primordial perturbations) for subsequent large-scale structure formation. When the field potential approaches its minimum, the inflaton decays into the standard model particles filling the Universe with matter that follows the metric's primordial perturbations (adiabatic initial conditions). The details of the shape of the inflaton potential drive the physics of the early Universe, particularly, how strong tensor modes are compared to scalar modes. The tensor-to-scalar ratio "r" drives the energy scale at which inflation occurs (r=0.01 typically corresponds to 10^{16} GeV, a possible particle physics unification scale, providing a direct link to high-energy physics beyond the standard model).

Inflation appears to elegantly and naturally solve these fundamental questions but it also raises new ones such as why the field was excited initially (how inflation started), and where this field came from. This is a usual situation in physics when one pushes the theoretical framework one step deeper. Being convincing and elegant is not sufficient for being true and one needs to have clear evidence that inflation occurred. While flatness and homogeneity cannot be taken as evidence for inflation for the theory was precisely built to explain them, there are clear observations in favor of inflation:

- The scalar spectral index n_s, measured with the CMB to be less than, but close to 1 with high confidence. This is a non-trivial prediction from inflation.
- The presence of multiple harmonics in the CMB power spectrum [12, 1], as well as the observation of Baryonic Acoustic Oscillations in the matter distribution [13, 14] shows synchronicity of the primordial perturbations, as in the case of inflation, and not continuously as from topological defects [15].
- Harmonics in the CMB T and E-polarization angular power spectra are in phase opposition [16, 17]. This is evidence for the adiabatic nature of the primordial perturbation, pointing towards inflation.
- Primordial non-Gaussianities are not observed in the matter distribution of the CMB [18], This is the sign of a highly Gaussian primordial perturbation generation process, a further argument for inflation.

If these observations altogether give a certain level of confidence throughout the community that inflation occurred, we're still missing direct evidence. Primordial B-modes in the CMB are the most promising probes as these can only be created by primordial tensor modes (equivalent to primordial gravitational waves) which are a non-trivial prediction from inflation. Their detection would exclude several alternative models such as the ekpyrotic model [64, 65] or semiclassical gravity [66] which predict r~0. Furthermore, the amplitude of tensor modes, and the scalar and tensor spectral indices n_s and n_t provide critical information about the physics of inflation. There exists a generic consistency relationship $r = -8n_t$ among a large class of inflationary models and combining these parameters allows reconstructing the actual shape of the inflation potential which is a direct measurement of early-Universe physics [10]. For these reasons, the detection and characterization of primordial B-modes are considered the *smoking gun* for inflation and are subject to intensive observational activity. In addition, they would confirm that the tensor perturbations, which only contain metric degrees of freedom, are quantized, a non-trivial result for quantum gravity [67]. Current best limits on the value of "r" were obtained by combining data from BICEP-KECK ground-based observatory (located at the South Pole) with the Planck Satellite data reaching $r < 0.036$ at the 95% C.L. [69].

Detecting the CMB B-mode polarization: a considerable observational challenge

While the scientific motivation for detecting B-modes is clear and exciting, it is an ambitious challenge for two main reasons: Instrumental limitations (sensitivity, systematics) and astrophysical foregrounds, which both make the signal interpretation complex and require sophisticated technologies.

A CMB polarimeter directly measures the Q and U Stokes parameters, that fully characterize linear polarization, by differencing the measured power from two orthogonal polarizations for Q (the same at 45° for U). These observables can be transformed by data analysis into the theoretically meaningful E and B modes through decomposition in a curl-free (even parity) and rotational (odd parity) modes respectively. The angular power spectra of these fields can be reconstructed and the primordial B-modes can be discovered through two main features: The reionization peak on the large scales (requires almost full sky coverage), and the recombination peak at degree scales (the most favored probe). The B-mode spectrum is expected to decrease at smaller scales with a slope given by n_t. The B-mode quest is challenging as the B-mode signal is very weak in absolute value (a few tens of nK at most) and much smaller than the E-modes and temperature fluctuations (respectively measured around 1 and 30 μK). This poses two major issues for detection:

1. Such a small signal can only be detected by extremely low-noise detectors, with intrinsic noise (mostly thermal) of the order or below the photon noise of the incoming radiation. Such detectors operate at sub-Kelvin temperatures. Given their typical sensitivity, arrays of thousands of detectors are needed to reach the B-mode sensitivity within a reasonable time making the instrument complex. The depth of a map is measured by its temperature noise RMS per resolution element in μK.arcmin. The typical depth required to improve on current constraints [69] is below a few μK.arcmin.
2. The amplitude hierarchy between T, E, and B is also problematic because E and B are measured from the observables Q and U, and any instrumental systematic will result in mixing between the original Stokes parameters, resulting in significant leakage of E into B-modes. For B-modes corresponding to r=0.01, cross-polarization needs to be lower than 1.5% for the leaked E-modes not to overcome the primordial B-modes. Instrumental systematics, therefore, need to be controlled in an unprecedented manner.

Incoming atmospheric background radiation (mostly water vapor in the atmosphere) has to be minimized. Satellites are optimal in that regard but due to cost and timescales, they tend not to be the first to measure but rather provide legacy high-quality measurements. Balloon-borne experiments benefit from a low atmospheric background but the duration and success rate of the flights are not yet sufficient to easily reach the required sensitivity. Ground-based experiments appear as the best compromise as they can extend over long periods and benefit from successive sensitivity and technological upgrades. They need however to be installed at dry, stable-atmosphere, high-altitude sites with related logistical complications. Currently, Antarctica and the Andes high plateaux (Atacama in Chile, Puna in Argentina) offer the best sky quality.

Regarding the control for instrumental systematics, the detailed design of the instrument can be a game-changer. Two main types of astronomical instruments have been used so far for CMB polarization:

- Imagers form an image of the sky on a focal plane equipped with cryogenic low-noise detectors such as background-limited bolometers. A polarizer and possibly a polarization modulator (such as a rotating Half-Wave-Plate) are used to build Stokes parameters maps and the T, E, and B power spectra. Because the wavelength is of the order of the typical size of the mechanical parts of the imager, there is significant diffraction in the optical chain resulting in a mixture of on- and off-axis signals at the detector stage. This can be the source of cross-polarization unless it is entirely within a cryogenic box.
- Interferometers use amplified signals from antennas and correlate them in pairs. The signals are multiplied using a correlator to produce fringes (the observable is the amplitude of the fringes, known as *visibilities*). The amplifier noise limits the sensitivity of interferometers while the cost and narrow bandwidth of the correlators increase the cost of a B-mode-sensitive interferometer. The observation of interference fringes allows for extra control of systematics in comparison with an imager [19, 20] using the method known as self-calibration. This contributed to interferometers being the first to measure sub-degree anisotropies [21] and E-mode polarization [22, 23].

With QUBIC, we propose using an alternative technology, Bolometric Interferometry, which takes advantage of sensitive imaging using large arrays of Transition-Edge-Sensors[1] to measure interference fringes in the focal plane and hence benefits from the exquisite control of instrumental systematics made possible by interferometry.

[1] Bolometers using the superconducting-to-normal transition as a high gain temperature to resistance detector.

Besides the smallness of the primordial B-mode signal, an even stronger difficulty appeared gradually over the past decade: Polarized foreground contamination by astrophysical sources that produce non-primordial B-mode radiation. These can be separated into actual sources of B-mode radiation (mostly from the Galaxy) and the effect of lensing that produces B-modes from E-modes:

1. After the Planck survey [24], it became clear that astrophysical foreground polarized emissions are brighter than the B-mode signal over the entire sky. Below ~100 GHz, these are dominated by the synchrotron emission, generated by cosmic-ray electrons spiraling around the Galactic magnetic field (the energy distribution of the electrons resulting in a Spectral Energy Density (SED) with spectral index β_{synch}~−3), while at higher frequencies Galactic dust emission dominates, caused by magnetized grains, heated by starlight and aligned with the Galactic magnetic field. The dust behaves like a ~18K gray body with emissivity β_{dust}~−1.5. The scenario is made even more complex by other emissions that could impact B-mode measurements. The anomalous microwave emission, for example, which is correlated with the dust and emits at low frequencies as a result of spinning grains [25], carbon-monoxide (CO) lines [26], which correlate with Galactic gas clouds, and extra-Galactic foregrounds generated by radio and infrared sources in a wide frequency range between one and several hundreds of GHz, with a brightness temperature that may decrease (radio sources) or increase (infra-red sources) with frequency [27, 28]. A thorough analysis of multi-wavelength public data has shown that no sky region is clean enough from foreground contamination to allow a significant B-mode detection below r = 0.01 without foreground removal [29]. The only way to remove the astrophysical foreground is to rely on their distinct spectral behavior to the CMB and make measurements at several frequencies allowing for distinguishing and separating them with sufficient accuracy.
2. While CMB photons travel from the last-scattering surface to our observatories, they pass through gradually forming large-scale structures whose gravitational potential acts as a gravitational lens, slightly changing the radiation direction. Most of the effect occurs at redshifts around 2 to 4 and the RMS (Root Mean Square) deflection is 2.5 arcmin which is therefore not significant on the largest scales. On smaller scales, however, it induces mixing between the observed Q and U resulting in leakage from E to B-modes. The resulting lensing B-mode spectrum, therefore, adds to the primordial and foreground signal in such a way that below a fraction of a degree, primordial B-modes are the smallest contribution. At large angular scales, the sample variance from the B-modes adds significant uncertainty so that detection of primordial B-modes without delensing can be considered down to typically r=0.005. Delensing can be achieved through complex data analysis using external large-scale structure data and/or high angular resolution E-mode measurement (few arcminute scales and smaller). It is worth noting that B-mode lensing is itself of great cosmological interest as its measurement provides valuable information on neutrino mass and the number of species as well as on Dark Energy.

QUBIC offers a specific approach to astrophysical foregrounds through spectral imaging, allowing for higher spectral resolution and foreground contamination mitigation than is possible with wide-band observation.

Among the many ground-based projects currently working on B-mode observations, all of them (except QUBIC) have made the choice of direct imaging. Distinct technological choices have been made by different teams corresponding to different scientific objectives:

1. Large aperture telescopes (LAT) such as SPTPol [30] or ActPol [32] have arcminute angular resolution, mainly targeting a precise measurement of the lensing signal (for neutrino physics and Dark Energy) as the unavoidable atmospheric signal filtering significantly reduces their ability to measure angular scales many times larger than their angular resolution.
2. Small aperture telescopes (SAT) such as BICEP/KECK [69] or CLASS [34], with degree angular resolution, directly target the primordial B-modes and respectively achieved depths of ~3 and ~20 μK.arcmin with anticipated sensitivities of σ(r) 0.005 to 0.01 during the next few years.
3. Astrophysical-foregrounds-oriented projects such as QUIJOTE [25] or LSPE [35] aim at characterizing deeper the foregrounds, mostly on the synchrotron side.

Simons Observatory [31] will combine LATs and SATs and reach a depth of 2.6-6.3 μK.arcmin in 5 years. The balloon-borne instrument SPIDER [60] flew in 2015 reaching ~20 μK.arcmin. All of these projects are imagers, some of them using polarization modulators and all with multiple wide-band frequency channels for mitigating astrophysical foregrounds. Besides these current projects, a global international effort called CMB-S4 aims at joining efforts with a range of small and large-aperture telescopes with many wide-band frequency channels, common designs, and observing strategies to address in a single collaboration all the

complexity of the B-mode search. CMB-S4 is US-led and plans to start observations in 2027 from Chile and the South Pole. A large-scale-oriented satellite LiteBird [61] is planned by Japan for a launch in 2030.

QUBIC uses the new technique of Bolometric Interferometry at ½ degree angular resolution using QUBIC for targeting primordial B-modes. We will rely on our original optical design and self-calibration for **instrumental systematics mitigation** and our unique ability to use spectral imaging for **astrophysical foreground mitigation**. Bolometric Interferometry allows for **high sensitivity with fewer detectors than classical imagers**. End-to-end simulations project a **competitive depth of ~1 to 3 μK.arcmin (respectively at the recombination peak scale ℓ~75 and at ℓ~400 [48])**. We expect to achieve a **conservative upper limit on r of σ(r)=0.015 [48] and as low as σ(r)=0.007 including all correlations as well as Planck data**.

Bolometric Interferometry and QUBIC

QUBIC is based on Bolometric Interferometry. This new concept combines the sensitivity of bolometric detectors with the instrumental systematics control of interferometers and provides a bonus capability to perform spectral imaging: simultaneously reconstructing spatial and spectral information. The concept was initially proposed by P. Timbie and L. Piccirillo in 2001 who are still members of the collaboration. Two collaborations on both sides of the Atlantic (BRAIN in Europe, and MBI in the U.S.A.) started to develop the concept. The efforts of the two groups merged into the QUBIC project in 2008. QUBIC now regroups 130 collaborators from France, Italy, Argentina, Ireland, the U.K., and the U.S.A.

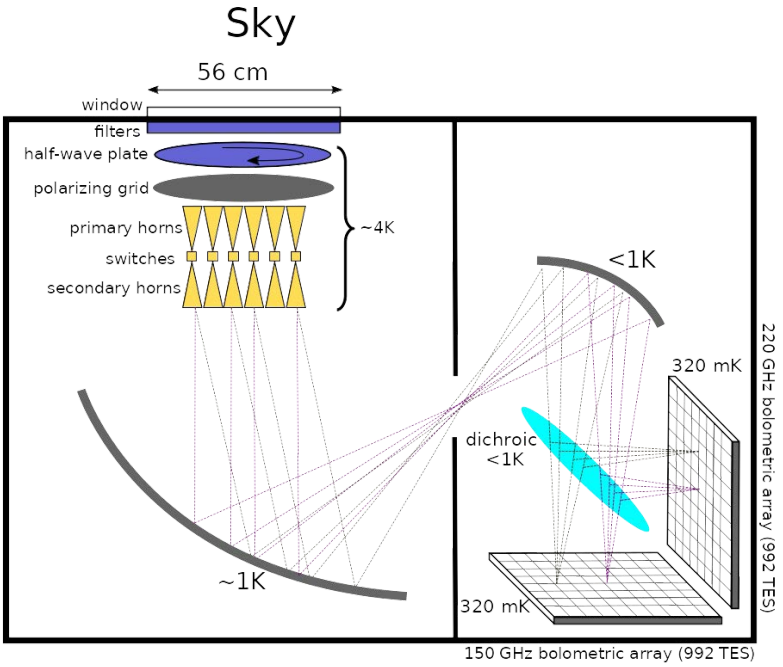

The concept of a Bolometric Interferometer is shown in the Figure on the right, our white paper [36], our Technical Design Report [37], or in the recent eight articles released in a JCAP special issue [38]. The signal from the sky directly enters the cryostat through a 40cm diameter window and a series of filters designed to cut high-frequency radiation that would bring background power in the cryostat [39]. The signal is immediately modulated by a rotating half-wave plate [40]. A polarizer is placed right after so that a single polarization is transmitted to the array of 400 back-to-back horns [41] (like pupils in a Fizeau interferometer) which directly illuminate two mirrors cooled down to 1K. This optical system [42] focuses the radiation from the horns onto two focal planes centered at 150 GHz and 220 GHz. The radiation from each horn is superimposed on the focal planes. As a result, the image in the focal plane is the sum of all the interference fringes corresponding to all baselines of the interferometer. These images are sampled by an array of 992 NbSi Transition-Edge-Sensors cooled down to 300mK [43]. Three major difficulties for B-modes search are addressed: Sensitivity, instrumental systematics, and astrophysical foregrounds:

Sensitivity:

Pairs of back-to-back horns act like pupils of a Fizeau interferometer forming fringes on the focal plane. Bolometers average the incident power over timescales longer than the EM-light period (time constants of tens of milliseconds). This is equivalent to performing optically the same operation as correlators do in classical interferometry. Contrary to classical interferometers, BI performs this over wide-band [44] and for a low-cost[2]. We have shown that wide-band and low bolometer noise allows a **Bolometric Interferometer to achieve a sensitivity comparable to that of a classical imager [45] with fewer detectors, as confirmed by our end-to-end simulations for QUBIC [48] and by our anticipated map depths given above.**

[2] In classical interferometry, wide-band is obtained by adding many narrow-band channels, with a huge consequence on the cost and complexity of the instrument.

Instrumental Systematics:

- Because we select a single polarization at the entrance of the instrument and our bolometers are purposely not polarization-sensitive, any cross-polarization occurring in the horns or the optical combiner does not affect our measurement. **QUBIC will exhibit a much lower level of instrumental cross-polarization than classical imagers, as has been confirmed during the QUBIC calibration campaign** (see Fig. 4 and [46])
- Because the observable of a Bolometric Interferometer is the fringe pattern from pairs of horns, it is possible to perform self-calibration [47]. This technique relies on the redundancy of baselines (pairs of horns in an interferometer array). In interferometry, a baseline corresponds to a Fourier mode on the sky. If it is redundant, the Fourier mode is measured multiple times with the interferometer so that the difference between these measurements can only arise from imperfections of the instrument. With parametric modeling of the instrument systematics, we showed in [47] that the corresponding nonlinear problem can be inverted and all parameters recovered by observing a polarized point source with all baselines successively. With QUBIC, we can measure individual baselines thanks to the use of switches placed in between the back-to-back horns that can be shut or opened individually [41]. A powerful millimeter calibration source (adjustable in frequency) will be placed at the top of a tower near QUBIC for self-calibration. **Self-calibration is one of the unique advantages of BI for controlling instrumental systematics.**

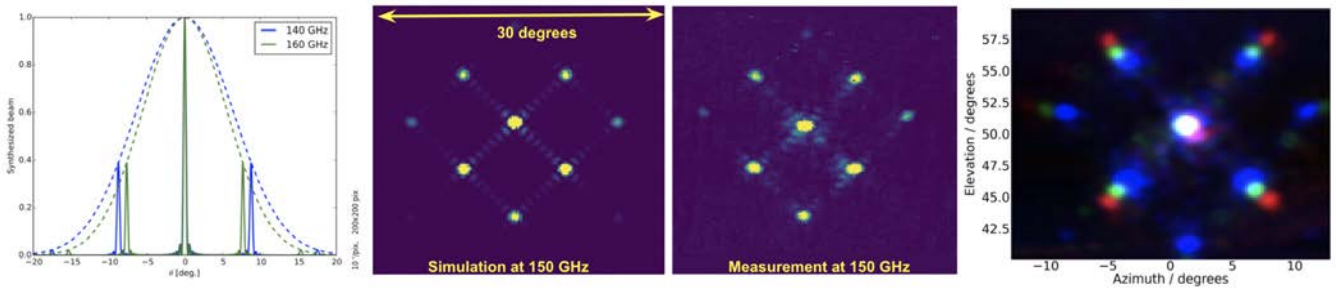

Figure 2. Left: cut across the synthesized beam (at 45 degrees) showing the multiple peaks and their primary beam envelope for two distinct frequencies. Center: 2D simulation of the synthesized beam (predicted in [36]) and measurement of the synthesized beam during the calibration campaign at 150 GHz [46]. Right false color image of the measured synthesized beam at 130 (red), 150 (green), and 170 GHz (blue).

Spectral Imaging and astrophysical foregrounds:

- The combination of all fringes from all pairs of baselines is the same as the synthesized image in classical interferometry. As a result, a Bolometric Interferometer performs images of the sky convolved by its beam, just the same way as a classical imager does. The main difference is that the beam of the Bolometric Interferometer is the synthesized beam formed by the relative locations of the 400 horns [42]. It has the shape of a series of regularly spaced almost-Gaussian peaks, each with a width given by the largest distance between horns while their relative spacing is related to the minimum distance between horns. The relative amplitude of the peaks comes from the primary beam of the horns (13 deg. FWHM). Fig. 2 shows a cut of the synthesized beam, as well as the full 2D predicted and measured synthesized beam at 150 GHz.
- The synthesized beam is the result of interferences that are heavily frequency-dependent. As a result, the shape of the synthesized beam significantly evolves with frequency. The multiple peaks shift from each other proportionally to wavelength. If the shift is larger than the width of the peak, the synthesized beam becomes different for this frequency, providing simultaneous spatial and frequency information. The result is the ability to do spectral imaging [48, 49]. This information can be used at the map-making step projecting the Time-Ordered-Data onto as many sub-bands as the wide band can fit sufficiently separated peaks in the synthesized beam. Within the wide band of QUBIC (25% bandwidth), we can resolve as many as five sub-bands, allowing QUBIC to achieve 5 times higher frequency resolution than a classical imager. **Spectral imaging is among the most important features of BI, opening the possibility of unprecedented constraints on the astrophysical foregrounds limiting primordial B-mode observations.** We have demonstrated the ability to perform spectral imaging with real data in the laboratory during the calibration campaign: setting the

source to 150 GHz, we reconstruct maps into 5 sub-bands and measured a maximum reconstructed brightness at this frequency while the measurements at all frequencies confirm our predictions for the spectral resolution (Fig. 3 and [46, 49]). Note that, in terms of noise, spectral imaging is nearly optimal [49], and because all detectors operate simultaneously at all N sub-frequencies, it achieves sqrt(N) better noise than usual Fourier-Transform Spectroscopy.

QUBIC site:

QUBIC observes from a clean-sky, dry-atmosphere (measured average emissivities 0.081 and 0.138 at 150 and 220 GHz [48]) site at 5000 m a.s.l. in the Salta Province (Argentina) with easy road access (45 minutes drive to the nearest city with a hospital, San Antonio de Los Cobres) allowing for access for maintenance all year long. A high-speed internet link to the city allows for remote control of the instrument and local technicians are there to perform regular maintenance of the instrument [68]. Installing an instrument in such a site is a challenge, but a part of the collaboration (Roma team) has extensive experience with installing and operating CMB instruments from remote sites (Antarctica, Svalbard). We have also hired technicians from local communities for on-site installation and maintenance.

QUBIC Status:

After a phase of R&D on subsystems, the QUBIC collaboration began building the Technological Demonstrator (TD) in 2016. The TD uses the same hardware as the Full Instrument (FI) but with fewer detectors (248 centered at 150 GHz instead of 992 in each of two focal planes centered at 150 GHz and 220 GHz), fewer horns (64 instead of 400), and smaller mirrors. It, therefore, has lower sensitivity than the FI but was an important step that demonstrated BI in the laboratory and will further be used to demonstrate it on the sky in phase 1. The TD was integrated and tested at APC, Paris, starting in mid-2018 and went through a detailed calibration and testing phase [46]. This fully confirmed all the predictions regarding BI. The most emblematic results are summarized in Fig. 2, 3, and 4. We have fully confirmed the predictions for the multiple-peaks shape of the synthesized beam (Fig. 2) and its evolution with the frequency which is the first step of the validation of spectral imaging. Spectral imaging into 5 sub-bands has been demonstrated with real data exhibiting perfect agreement with the expected spectral resolution (Fig. 3). We measured the intrinsic cross-polarization (Fig. 4 left) of the instrument to be less than 0.3% at 95% C.L., well below our competitors, validating our optical design optimized for low cross-polarization. We have also successfully used the shutters to observe individual interference fringes (Fig. 4 right) which is the first step in the validation of self-calibration. Finally, we combined all the calibration steps and built a pipeline to reconstruct a map of our calibration source (Fig. 3), involving full mapmaking with the multiple peaked synthesized beam, and obtained the map of a point source with the expected angular resolution. The calibration phase was concluded by a review organized in January 2020 by CNRS/IN2P3 with the participation of INFN. The panel highlighted the innovation of this first-ever Bolometric Interferometer, assessed the concept's capabilities as excellent, and found the spectral imaging feature of utmost utility for foreground control [50].

The shipment to Argentina was delayed due to COVID. The instrument safely arrived in Salta on July 18th, 2021, where validation tests were conducted in the integration hall built for QUBIC in Salta City. The first cryogenic cooldown started on Aug. 18th, 2021, only a month after the arrival of the container, demonstrating the instrument to be operational after transportation.This was a major achievement especially since we relied entirely on local teams, videoconferences, and extensive documentation because Argentinean borders were closed due to the pandemic. Testing and the training of local teams continued in Salta with a successful observation of the Moon in July 2022, which allowed for the first measurement of the Moon EM spectrum using spectral imaging with Bolometric Interferometry (see Fig. 5).

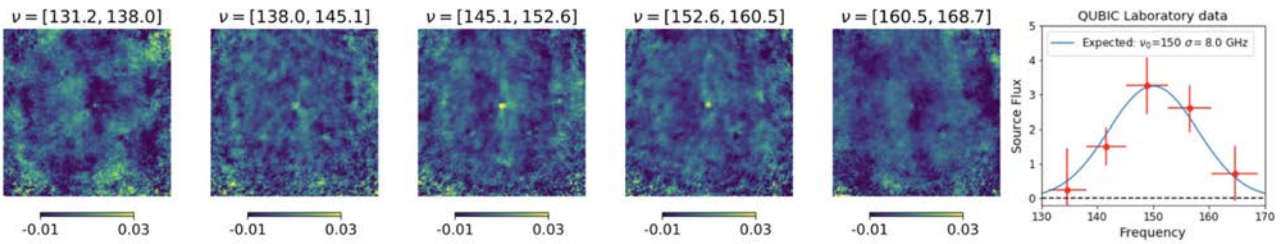

Figure 3. Reconstructed images of our artificial calibration source using spectral imaging in 5 sub-bands. The source was set to 150 GHz. The measured intensity of the source is shown on the right as a function of frequency (red points) while the expected spectral resolution (8 GHz) is superimposed in blue (no fitting) [46, 49].

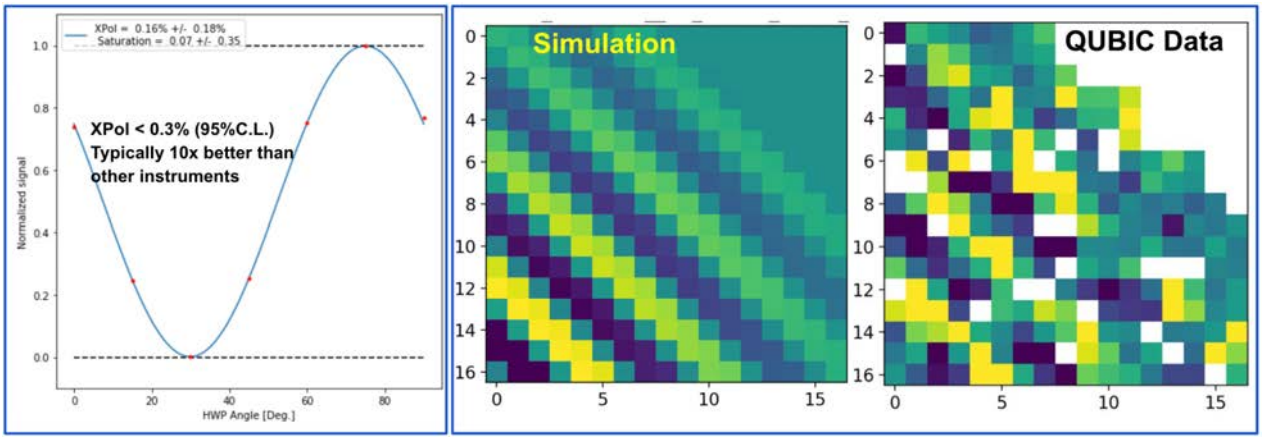

Figure 4. QUBIC Calibration campaign results, (together with Fig. 2 and Fig. 3). Left: cross-polarization measurement about 5 times better than other instruments. Right: Individual fringe on the focal plane.

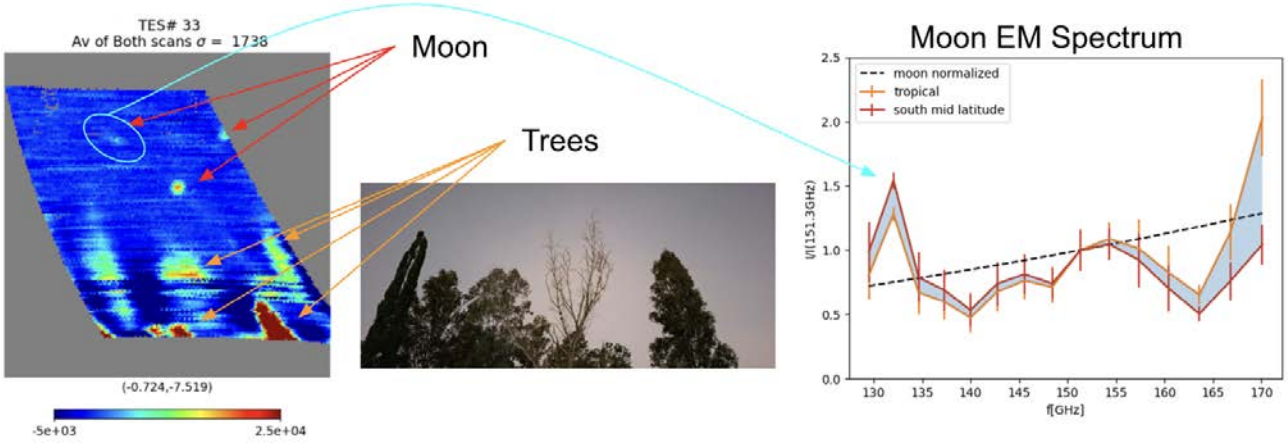

Figure 5. QUBIC observations of the Moon from Salta (July 2022). The Moon appears in the left coadded image with multiple replications corresponding to the Synthesized Beam (see Fig. 2), we also see multiple replications of the trees present in front of the door of the Integration Hall. A study of the frequency shift of the Moon secondary peaks using multiple TES allowed for the first measurement of the Moon EM spectrum using Spectral-Imaging (right image) [71].

QUBIC was installed at the site in October 2022 with the inauguration happening on Nov. 23rd, 2022 (see Fig. 6). A number of technical issues related to the site itself resulted in a slow start of the commissioning: leaks of the Dome resulting in melted snow leaking on the electronics, mechanical issues with the dome itself as well as the need for a global redesign of the electrical installation. The commissioning of the instrument could only really start in April 2023 and has been progressing since then. So far we have successfully performed the following operations remotely (controlled from Buenos Aires and/or Paris): cooldown the instrument, cycle the fridge operate and tune the TES, detect the signal from both our calibration source and internal carbon fibers, as well as perform a number of sky-dips (see Fig. 7) that demonstrated a much colder temperature of the sky with respect to the QUBIC dome (as expected). More detailed commissioning results will shortly be available, as well as first Moon and sky observations from the observing site.

Figure 6. QUBIC at the site (5000m a.s.l.) during the inauguration on Nov. 23rd, 2022.

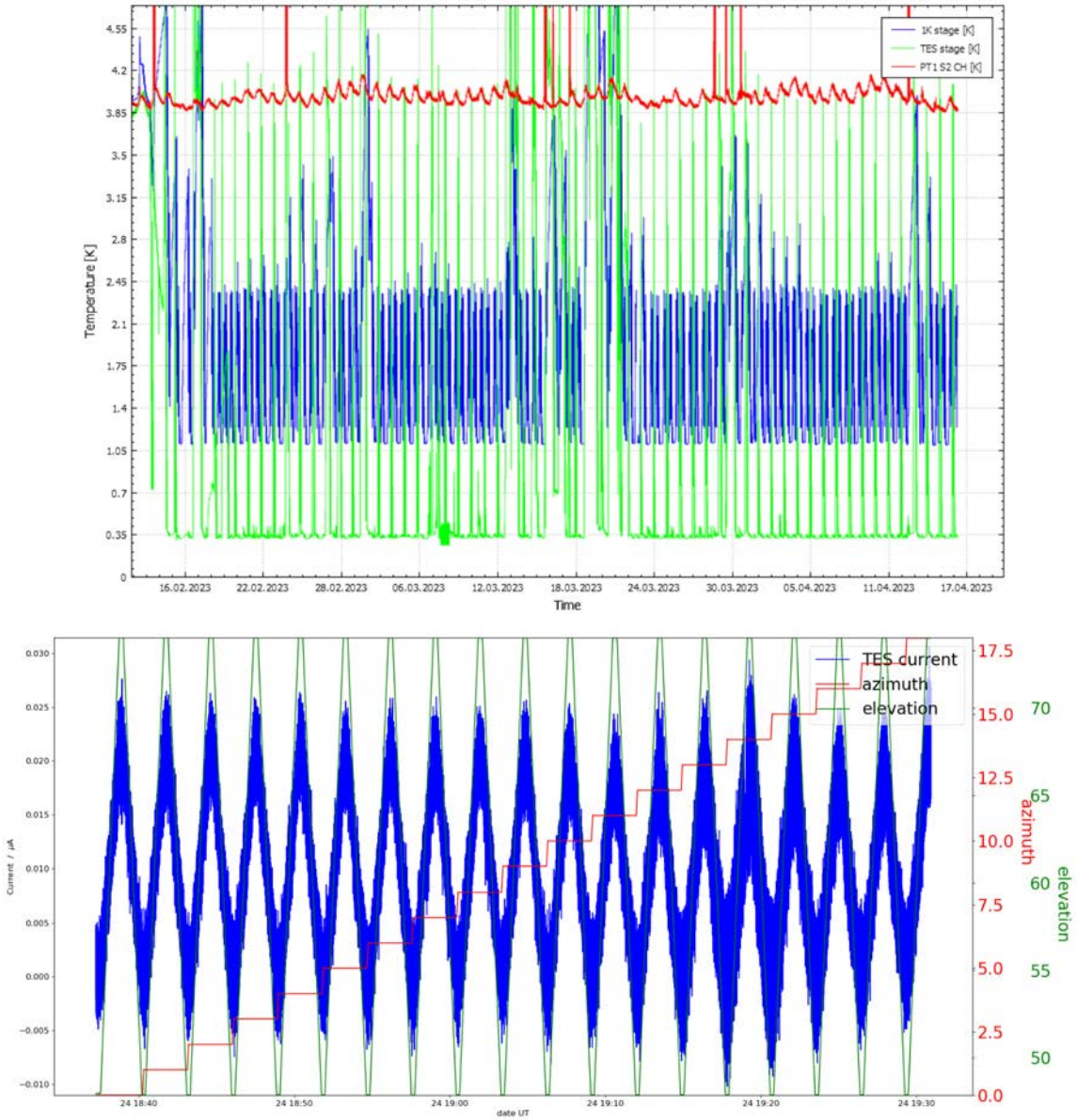

*Figure 7. Data from the QUBIC commissioning: **(top)** temperatures of the cryogenic stages since Feb 2023. We achieve a cryogenic yield of 50% of the time (focal plane at nominal temperature of 350 mK). **(bottom)** Sky dips from the QUBIC site. The measurement was done multiple times at different azimuth pointing directions. Note the correlation between elevation (in green) and the bolometer data (in blue) demonstrating our sensitivity to the sky emission.*

QUBIC timeline

We plan to exploit QUBIC to produce cutting-edge results on the measurement of the B-mode polarization of the CMB over five years starting with on-site operations of the TD, involving two scientific phases corresponding to two successive upgrades of the instrument. **This program will achieve a map depth of 1 to 3 µK.arcmin (from ℓ~75 to 400) corresponding to a conservative sensitivity σ(r)=0.015 [48] for QUBIC alone after 5 years (σ(r)=0.007 including all correlations and Planck data).** In the following, we describe the QUBIC schedule (including upgrades), the 2 scientific phases, the work packages for this ambitious objective to be reached, and a risk analysis.

The two successive phases for QUBIC correspond to each configuration of the instrument and each with specific scientific objectives (see Fig. 8 for a schematic view of the phases).

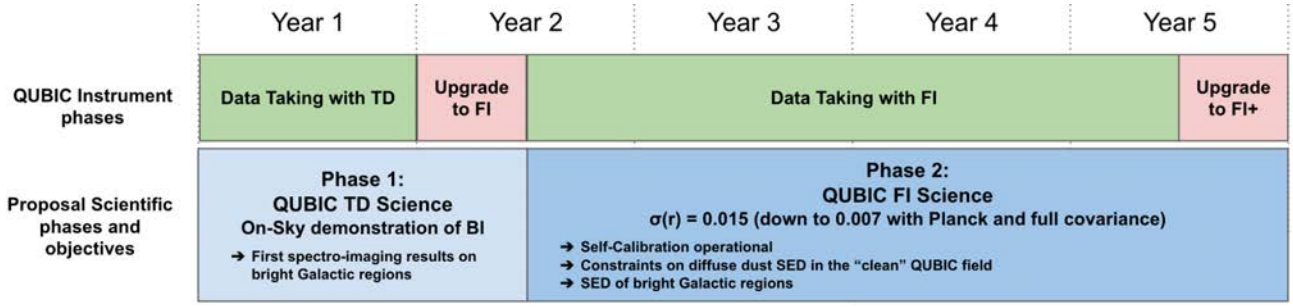

Figure 8. Timeline of the two phases of QUBIC instrument phases and personnel resources.

Phase 1: On-sky demonstration of BI and Spectral Imaging with the QUBIC TD

This phase will start 6 months after the installation and commissioning of QUBIC. The dataset will be 1 year.

The objective of this phase, besides validating BI will be to demonstrate spectral imaging with BI on sky data [48]. QUBIC will focus observations on bright Galactic regions during this phase to optimize the scientific return from the moderate sensitivity and angular resolution (1 degree) of the TD. We aim to obtain SED measurements of well-known Galactic regions with QUBIC and compare them with previous measurements (see Fig. 6 for a forecast for phase 1).

The Data Analysis activities for this phase will first be cleaning the Time-Ordered-Data from any housekeeping signal, filtering-out atmospheric contamination, and producing clean TOD to be used for map-making. In parallel, calibration of the detailed synthesized beam shape and frequency evolution, as well as preliminary self-calibration, will allow improvement on the first map-making attempts to be able to produce spectral imaging maps of the target regions as forecasted in Fig. 9. **Obtaining spectral imaging data on various Galactic regions will be a new result in itself and will lead to several publications. We also plan to observe the Moon extensively and achieve a detailed EM spectrum measurement as was initiated in Salta (see Fig. 5).**

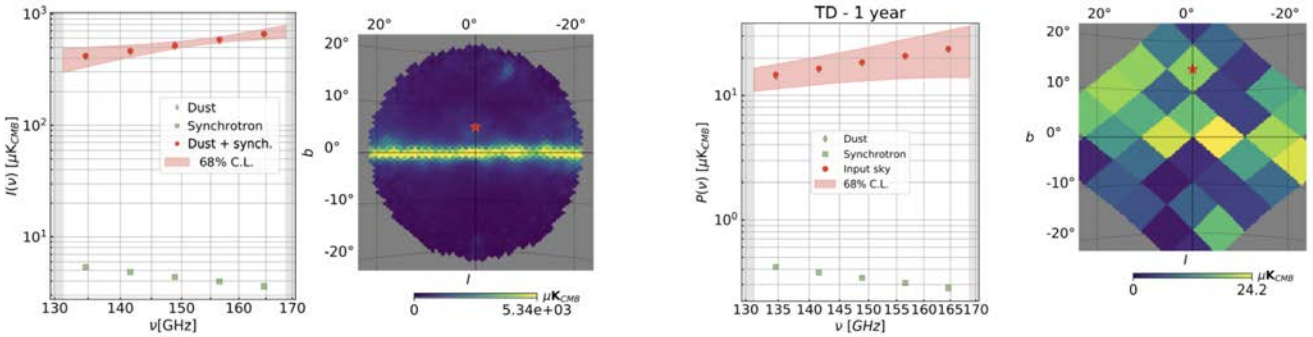

Figure 9. Forecasts for Spectral-Imaging measurements (5 sub-bands, light-red region) with the TD [48] in total intensity (left, 1deg. resolution) and polarization (right, 7.3 deg. resolution). The SED is that of the pixel with a red dot.

After 12 months of operations with the TD we will proceed to the upgrade to the FI. This implies replacing the current 64- horns array with the 400 version that is already fabricated and measured to match

requirements, replacing the small mirrors with full-sized ones that are also fabricated and measured to match requirements, and equipping the two focal planes with TES arrays that still need to be manufactured with no change to the current ones that match the requirements. After this, **QUBIC will reach its nominal sensitivity**. The upgrade corresponds to a sensitivity improvement of factor 30 considering the number of horns and detectors for the TD[3]. The gain in angular resolution will be a factor 2 reaching 30 arcmins.

Phase 2: QUBIC FI Science - Measurement of B-mode polarization down to σ(r)=0.015 (conservative)

This phase will start with the commissioning of the FI, relying on the experience acquired with TD. The dataset for this phase will be 3 years.

Full end-to-end simulations were conducted (assuming stable atmosphere in Argentina, no instrumental systematics residuals) with the expected FI noise from the TD measurements [48]. Spatial noise anti-correlation is induced by the synthesized beam multiple peaks deconvolution performed during the map-making (Fig. 10 left) and results in a significant noise reduction with respect to white noise at scales corresponding to the angular distance between peaks (ℓ~50-100) giving QUBIC enhanced sensitivity at the recombination scale (Fig. 7 center). **Our map depth (for 150 and 220 GHz) is 2.7 and 3.7 μK.arcmin at ℓ~400 and reduces to ~1 μK.arcmin at ℓ~75 [48].** A likelihood analysis for the primordial tensor-modes, not including Planck data, neglecting off-diagonal terms in the covariance matrices, assuming no foreground subtraction residuals (hence corresponding to our sensitivity to "effective-r") achieves a **conservative sensitivity σ(r)=0.015 combining our two bands [48]. Including Planck and off-diagonal covariance improves the sensitivity to σ(r)=0.007.**

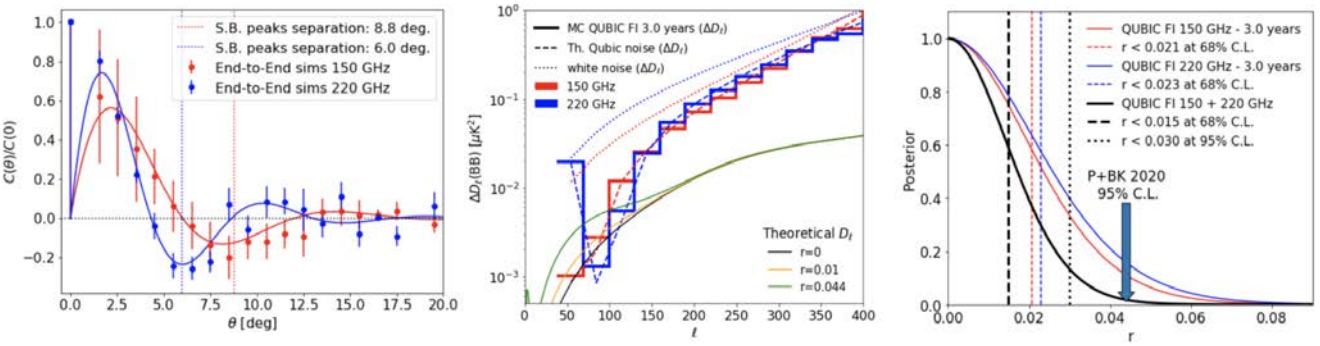

Figure 10. Left: noise anti-correlations induced by multiple-peaks deconvolution. Center: Error bars on the BB power spectrum from (solid lines) compared with theoretical expectations for QUBIC (dashed) and white-noise (dotted). Right: Conservative-Likelihood analysis on r assuming perfect foreground subtraction showing our sensitivity σ(r)=0.015 [48] (when including Planck data and full noise covariance matrix, we achieve σ(r)=0.007).

The main objective of this phase will be to constrain B-mode emission in the clean BICEP2 sky patch using QUBIC in both full-band and spectral imaging modes around 150 and 220 GHz as forecasted above and shown in Fig. 7. We are willing to achieve a detailed characterization of the foreground in this patch by measuring its spectral and spatial characteristics using multiple sub-bands within our two spectral bands and various component separation techniques. The second objective of phase 2 will be to map in spectral imaging mode several regions of interest (similar to those in Phase 1 but with improved sensitivity and angular resolution) and measure their SED [48]. Such observations near the Galactic plane or in low-dust emission regions are forecasted in Fig. 11. It illustrates how we can directly observe the amount of dust present in our "Primordial B-modes" patch (dust emissions from PySM3 [52]).

The unique ability to control dust contamination with BI is illustrated in Fig. 12 (left) where we have assumed imperfect dust removal at 220 GHz (our most sensitive channel because slightly multimoded) resulting in an effective "dust *r*" of 0.05 (around the current best upper-limit) when measured in the full band. Through spectral imaging with 2 sub-bands (corresponding to 3 inter-band cross-frequencies), we show that the recovered values of *r* evolve with frequency (blue points), detecting the slope at 2.9σ level with 3 years of data. If the *r* measured in the full-band was due to primordial tensor-modes, we would find a flat frequency evolution within the band (red points). This specific simulation illustrates the specific power of spectral imaging in controlling foreground contamination in a way that is not achievable with a classical

[3] as well as residual excess noise observed in the TD detection chain (noise aliasing) that will be fixed for the FI.

imager. Indeed they can only do this kind of analysis between wide, largely separated bands (90, 150, 220 GHz) and not in a local fashion within the physical band. In the eventuality of "dust decorrelation" [53, 18] widely separated bands do not bring relevant information on dust, while local SED can detect such an effect.

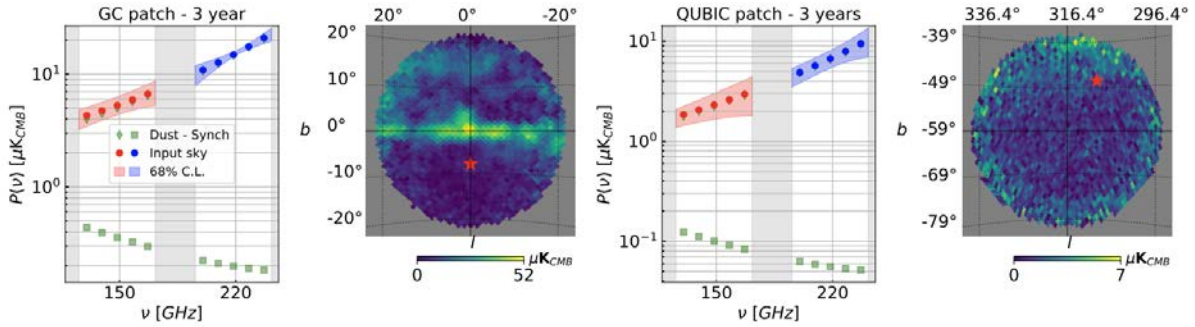

Figure 11. Forecasts for Spectral Imaging measurements (5 sub-bands, light-red region) with the FI [48] in polarization (1 deg. res.) mear the Galactic plane (left) and the Clean BICEP2 patch (right). The SED is that of the red dot pixel.

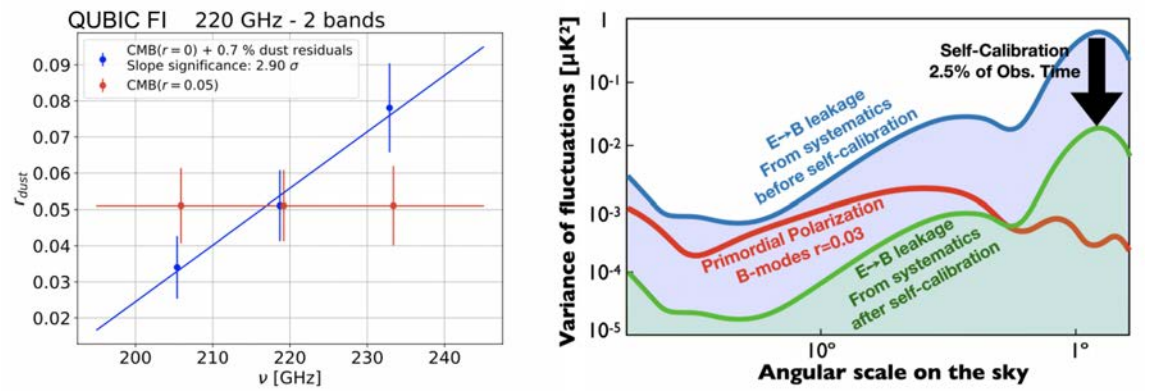

Figure 12. Left: Spectral imaging distinguishes dust residuals from tensor- modes at the 2.9σ level within the band [48]. Right: Self-Calibration forecasts from [47]. We simulate the E→B leakage from realistic systematics resulting in the blue measured spectrum. With 2.5% of the time on self-calibration, the effect is reduced down to the red level

A wide number of topics will have to be investigated during this phase:

- Continuation of TOD analysis and map-making improvement, including spectral imaging
- *Self-Calibration*: establishing self-calibration at the full QUBIC scale will require significant development. We will build and fit the parameters of a model describing the various systematics from the instrument as described in [47]. With this advanced model of the instrument, map-making and spectral imaging will be more accurate and only residuals from this systematic effect modeling will remain in the final maps. We have shown that spending 2.5% of the observation time on self-calibration will reduce systematics by an order of magnitude (see Fig. 12 right panel). This allows finding a balance between the magnitude of the systematic and statistical uncertainties in our data products.
- *Pure angular power spectrum estimation*: These techniques intend to minimize the effect of the cut-sky when calculating E and B mode spectra from an observed map[4]. Several techniques can be investigated here beyond the classical one (pseudo-power spectra using NaMaster [51]) that was used for the forecasts presented here. These include the maximum-Likelihood approach which can be very efficient on the largest scales as well as a new technique we have started to develop based on Machine-Learning.
- *Component separation*: We will consider three different flavors for component separation, two of them are classical (frequency-maps based and frequency-spectra based). The third is only achievable with a Bolometric Interferometer and fully uses the spectral imaging capabilities. The idea is to directly perform map-making per component instead of map-making per frequency (see next section).

[4] On a partial sky the spherical harmonics are no longer a complete basis, resulting in E to B leakage.

New possibilities from Spectral Imaging with QUBIC

This section describes very recently discovered new tracks offered by spectral imaging that illustrate how Bolometric Interferometry is a potential game-changer in CMB Polarization observations, especially from the foreground control point of view, but also from the instrumental design point of view.

Ultra-Wide-Band instrument

the possibility of performing spectral imaging has already been successfully demonstrated with a monochromatic artificial source in the laboratory (see Fig. 3) and on the sky with the Moon which is a wide-band source for which we could measure the spectrum, although with still large uncertainties as it was obtained from Salta City where the atmosphere is very emissive. We also have performed extensive simulations with the CMB including foregrounds (see [49], Fig. 9, 11, 12 as well as articles in preparation [72] and [73]).

This technique is so promising that we are considering the possibility of considerably simplifying the QUBIC focal planes design for the Full Instrument by removing one of the two focal planes and using a single focal plane for observing from 130 to 250 GHz. This is known as the Ultra-Wide-Band design (UWB). Such a design requires the use of a “notch filter” in order to strongly suppress the frequencies from 180 to 195 GHz where a strong water emission line is present and would result in significantly higher noise if not filtered out.

From the effectiveness point of view, this possibility is appealing as the cost is heavily reduced by having a single focal plane (the most costly subsystems in QUBIC are the superconducting cryogenic readout cables whose number is reduced by a factor 2 in this novel design). Noisewise, we expect a slight gain due to the fact that the detector intrinsic noise only happens once instead of happening for both focal planes in the classical design. Atmospheric noise is however much higher in the 220 GHz band than at 150 GHz and a worry was to see the photon noise from high-frequency degrading significantly the performance of the 150 GHz part. This consideration is mitigated by the fact that our feedhorns are multimoded at 220 GHz. This is because we use the same physical horns from 150 GHz, where they are single-moded, to 220 GHz where more modes propagate due to a smaller wavelength. As a result, our signal-to-noise ratio at 220 GHz is slightly better than at 150 GHz as already demonstrated in [42] and [48] and visible in Fig. 10 (middle and right panels).

In the framework of Mathias Regnier’s PhD thesis, we have performed extensive simulations based on spectral imaging and we demonstrate that the sensitivity is not affected, and is even slightly improved in such a design because of the single occurrence of the detector noise. With an improved version of the frequency map-making based on spectral imaging and including external data (Planck frequency maps) in order to regularize edge effects that were increasing our noise in [48], we find a sensitivity to primordial B-modes of $\sigma(r)=0.01$ with the initial dual band design and $\sigma(r)=0.009$ with the single focal plane UWB design.

We have obtained funding from University Paris Cité to purchase the Notch Filter from Cardiff University which can manufacture it without any particular technical difficulty.

We want here to emphasize the fantastic perspectives offered by this new approach. In a classical imager, the whole focal plane is not populated with detectors sensitive to the whole frequency range required to perform foreground mitigation. In the best case, one uses dual-band bolometers, but this is not the case for all current or forecasted instruments. With our Ultra-Wide-Band approach, each square centimeter of the focal plane can be sensitive to all frequencies of interest, the band splitting is performed at the data analysis level using spectral imaging and achieves a factor 5 better spectral resolution as already demonstrated with QUBIC. For a similar budget, this corresponds to a gain in sensitivity of a factor of a few (depending on the exact configuration) while using very simple detectors sensitive to the whole bandwidth (as bolometers naturally are).

Component Map-making

Spectral imaging relies on the fact that the synthesized beam of a bolometric interferometer such as QUBIC is highly sensitive to frequency (see Fig. 2). So far we have presented spectral imaging as a way to reconstruct sky images in sub-bands within the physical band of the instrument. Then, similarly as with a classical imager, one can perform component separation in order to clean the CMB maps from the presence of Dust, Synchrotron or other contaminants (such as CO emission for instance). Such an approach has been

extensively explored with imagers and appears successful, but the actual modeling of the noise in the maps can complicate matters in a significant manner if spatial noise correlation is present in the maps, which can happen due to atmospheric fluctuations for instance.

However, with a bolometric interferometer, the frequency-maps step appears as unnecessary because of the direct frequency dependence of the TOD. One can directly incorporate the component separation inside the mapmaking, avoiding complex modeling of the noise in the maps, only relying on the time-domain modeling of the noise, which is more straightforward. Our map-making techniques operate through an "inverse problem" approach by simulating frequency sky maps and passing them through a series of massively parallelized operators modeling in a detailed manner each stage of the instrument in order to produce the time-ordered data simulated from this trial set of sky maps. A cost function is then minimized in time domain through a preconditioned conjugate gradient that allows to update the input simulated sky maps through a number of iterations, eventually achieving an unbiased estimate of the input frequency sky maps. It is then straightforward to update this algorithm so that it starts from Astrophysical Components maps and a mixing matrix parametrizing the way sky components are mixed at each frequency according to their EM spectrum. Unknown parameters in the mixing matrix can be estimated along with the estimate of the sky maps by minimizing the exact same time-ordered-data cost function.

We have successfully implemented such a "components map-making", in the framework of Mathias Regnier's PhD thesis, using a parametric approach where the actual frequency behavior of the astrophysical components is modeled (using a modified black body with a sky-varying spectral index for the dust for instance). Our algorithm makes it straightforward to incorporate external data sets, such as Planck sky maps at various frequencies, in order to provide an additional frequency lever arm to the component separation. We obtain an unbiased reconstruction of the sky components, even in the presence of synchrotron emission and CO emission lines as shown in Fig. 13.

This new technique will be published shortly [73] and will also include a non-parametric method on which we are also currently working.

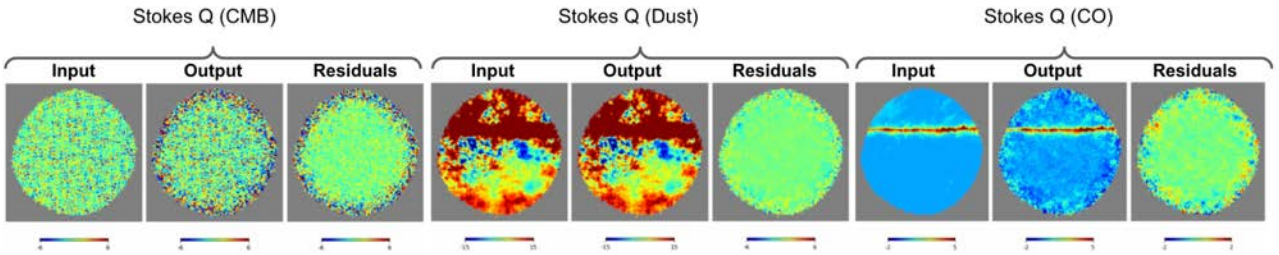

Figure 13. Component map-making result (Q Stokes parameter): we have used an input sky including CMB, Dust with a sky varying spectral index (d1) and the CO emission line. For each component we show the input sky, the reconstructed obtained directly from the components map-making (TOD -> Components) and the residuals.

Detecting Dust Decorrelation with Spectral Imaging

The recent history of CMB B-modes search has demonstrated that Galactic Foregrounds are more complex than anticipated. This led the BICEP2 collaboration to a wrong discovery announcement in 2013 and one certainly does not want to experience the same. It is therefore of paramount importance to make sure that our idealized assumptions on the spatial and frequency behavior of Galactic Foregrounds will not lead to unaccounted residuals in the clean CMB maps nor erase actual primordial B-modes.

Galactic dust is usually assumed to follow a modified black body EM spectrum:a black body multiplied by a power law, whose spectral index has been measured to vary significantly across the sky. Forecasts for the tensor-to-scalar ratio sensitivity published by the various collaborations usually assume this model. It is however clear that such a model can only be a simplified version of reality as it is known that if the line of sight contains multiple dust clouds at different temperatures, this model does not hold.

A particularly complicated realistic dust model is one with frequency decorrelation of the dust emission. It arises from spatial variation of the dust spectral energy distribution (SED) over the sky and along the LOS due to the underlying structure of the Galactic magnetic field. In the presence of frequency decorrelations, the appealing forecasts for the sensitivity on r of the incoming projects end-up significantly degraded as can be seen in Fig. 13 (left) with forecasts for CMB-S4 with various dust models. If dust exhibits decorrelation (with an optimistic level lower than the current limits from Planck) the reconstructed r spans a wide range of values, well beyond the usually considered sensitivity of CMB-S4 (although this result is very clearly

explicited in the CMB-S4 forecast article [74]). In order to assess the possibilities of a Bolometric Interferometer for such complex dust models, we have performed the same forecasts, but assuming a BI design, allowing for spectral imaging, for CMB-S4 instead of that of a classical imager [70]. The middle panel of Fig. 13 shows the reconstructed *r* as a function of the number of frequency sub-bands used in spectral imaging. We clearly see how the ability to explore various numbers of sub-bands at the data analysis allows to identify the contamination by undetected foregrounds through a significant reduction of the bias on *r* when the number of sub-bands increases, while it would remain constant in the absence of such decorrelation or in the presence of real primordial B-modes. The left panel of Fig. 13 shows how one can efficiently perform a classification for a single realization between contaminated and not contaminated using a simple Machine Learning based classifier based on spectral imaging results.

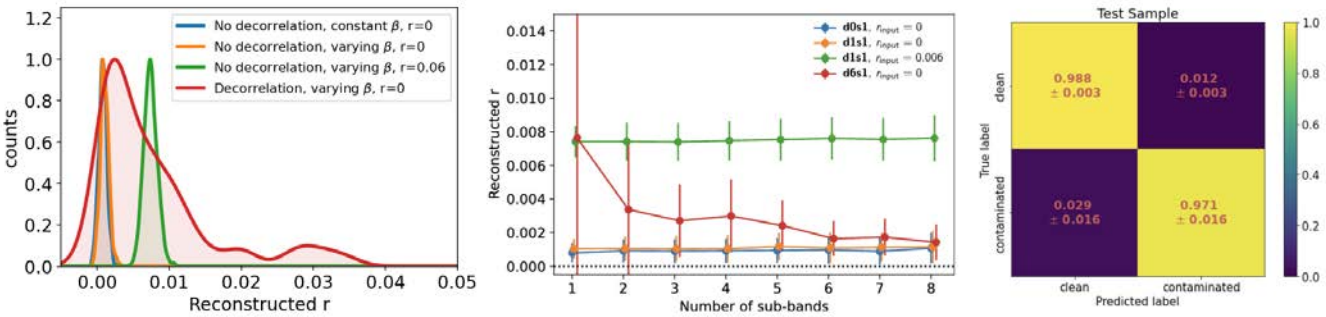

Figure 14. Dust decorrelation and spectral imaging with a CMB-S4-like instrument (see text). Figures extracted from Regnier et al., [70] (currently undergoing internal reviewing within QUBIC).

Atmospheric mapping with spectral Imaging

Atmospheric fluctuations are responsible for a significant sensitivity reduction with real data with respect to idealized forecasts for ground-based instruments, even from dry sites such as in the Andes or in Antarctica. A recent idea, inspired from the components map-making, is to add in the sky model, besides the (RA, Dec) sky components, an atmospheric template in local coordinates (Azimuth, Elevation) moving and evolving according to the winds. The morphology, time and spectral evolution of this template would correspond to additional unknowns to be estimated along the sky components using the same cost function in time-domain. This idea will be the heart of a PhD to start in October 2023 and seems feasible and likely to significantly improve the noise eventually achieved in the maps reconstructed from real, atmospheric contaminated data.

Perspectives: Bolometric Interferometry beyond QUBIC

The scientific motivation for searching for primordial B-modes is very strong, aiming at unveiling the physics of the primordial Universe and finding direct evidence for inflation. Observational difficulties make this a challenging objective (sensitivity, instrumental systematics, foregrounds). Several instrument designs have been proposed by various teams, each with specific advantages and drawbacks for solving the issues. The vast majority of the community has chosen direct imaging as the preferred design. They are gradually converging towards establishing the large CMB-S4 project with a number of small-aperture (large angular resolution for primordial B-modes) and large aperture (small angular resolution for lensing physics and B-mode delensing) telescopes. Such an extraordinary discovery as the tensor-modes from inflation will require extraordinary evidence and should not rely on a single technology especially because systematics (instrumental or astrophysical) can mimic the primordial signal. The Simons Observatory (SO) proposes a more gradual approach to the 2030 decade sensitivity by starting with a smaller number of telescopes and increasing to CMB-S4-like sensitivity through Advanced SO that has just been funded. A likely (and reasonable) future would be that those two projects would merge at some point.

The studies presented above show how Bolometric Interferometry could play a game-changing role in the quest for primordial B-modes, the understanding of the early Universe and tests for inflation and quantum gravity. The advantages and paradigm changes cover a wide range of aspects of CMB polarization studies:

- The possibility to build instruments covering a wide range of frequencies, with high spectral resolution and a reduced number of simply designed detectors (as they all cover all frequencies) opens the path to much cheaper instruments than currently anticipated, providing a higher level of control of instrumental systematics (thanks to self-calibration and a low cross-polarization design) and better foreground characterization, understanding and mitigation,
- the ability to identify contamination from foregrounds with a complex spectral behavior, which is expected from these realistic, large number of degrees of freedom, astrophysical emitters,
- fabricating components maps directly from time-ordered-data thanks to the synthesized beam frequency dependence completely unifies in a single step the CMB polarization data analysis, making it easier to achieve optimality by accounting more easily for noise covariance in time-domain rather than in map-domain.
- The possibility of projecting-out atmospheric fluctuations at the same time as one performs map-making, if confirmed and applicable, will undoubtedly increase the performance of a bolometric interferometer for a given “white-noise” sensitivity.

The QUBIC collaboration is convinced that BI has a significant role to play in the CMB-Polarization landscape with its unique approach to instrumental systematics and foreground contamination control. We believe that QUBIC should not compete but rather should join forces with CMB-S4 and/or SO and complement them with our innovative technology. This could happen through full integration in these collaborations in which QUBIC would be the leading European and Argentinean contribution, or through data-sharing agreements at later stages. The CMB-S4 instruments will not all be located at the same site with some in the South Pole and others in Chile. A common scanning strategy, file formats and shared pipeline make CMB-S4 a cohesive project across physical sites and instruments, which QUBIC could easily fit into. From the instrumental point of view, initial studies seem to indicate that fitting a bolometric interferometer into one of the cryogenic tubes of CMB-S4 or SO is likely to be possible with minimal hardware modification (a detailed design study is however clearly required) while Bolometric Interferometry could easily work with different detectors such as MKIDs as developed within IN2P3 in Grenoble.

Such a project could unite IN2P3 teams (and beyond) in an ambitious scientific program, joining the numerous fields of expertise present in our institute: instrumental design, detector technologies, data analysis and simulations. Considering the involvement of INFN in QUBIC it is also clear that such a project would come with high synergy with our Italian colleagues. The momentum coming from such a project might also trigger interest from other European groups, already involved in CMB-Polarization but finding it difficult to contribute collectively in a satisfying manner to the large US projects of the next decade. An ambitious, widely opened, Bolometric Interferometer could become the France-driven flagship project in Early Universe Science. **Bolometric Interferometry gives the opportunity to return France to the leadership role, acquired with Planck, in the science of the Cosmic Microwave Background and the Early Universe.**

References:

[1] Planck 2018 results. VI. Cosmological parameters submitted to A&A (2018)
[2] A. G. Riess et al. (Supernova Search Team), Astron. J. 116, 1009 (1998).
[3] S. Perlmutter et al. (Supernova Cosmology Project), Astrophys. J. 517, 565 (1999)
[4] P.A. Zyla et al. (Particle Data Group), Prog. Theor. Exp. Phys. 2020, 083C01 (2020)
[5] A. Ijjas, P.J. Steinhardt, A. Loeb, Physics Letters B, Volume 736, p. 142-146 (2014)
[6] A. A. Starobinsky, Phys. Lett. B91, 99 (1980)
[7] A. H. Guth, Phys. Rev. D23, 347 (1981).
[8] A. D. Linde, Phys. Lett. 108B, 389 (1982).
[9] A. Albrecht and P. J. Steinhardt, Phys. Rev. Lett. 48, 1220 (1982)
[10] Baumann et al., 2008, AIP Conference Proceedings 1141, 10 (2009);
[11] V.F. Mukhanov and G.V. Chibisov 1981 JETP Lett. 33 532
[12] G.F. Hinshaw et al., (WMAP) Observations: Cosmology Results Hinshaw, G.F., et.al., 2013, ApJS., 208
[13] L. Anderson et al., MNRAS, Volume 427, Issue 4, pp. 3435-3467.
[14] N.G. Busca et al., Astronomy & Astrophysics, Volume 552, id.A96, (2013)
[15] W. Hu, 197th AAS Meeting, id.32.01; Bulletin of the AAS, Vol. 32, p.1448 (2000)
[16] C. Prycke et al., ApJ, Volume 692, Issue 2, pp. 1247-1270 (2009).
[17] W. Hu and M. White, New Astronomy, Volume 2, Issue 4, p. 323-344 (1997)
[18] Planck Collaboration, Planck 2018 results. IX, A&A November 20, (2019)
[19] T. J. Cornwell and P. N. Wilkinson, MNRAS196 (1981) 1067
[20] Pearson and Readhead, Ann. Rev. Astron. Astrophys.22 (1984) 97
[21] Scott et al., 2002, MNRAS 341(4):1076 - 1083 (2003)
[22] Readhead et al. 2004, Science, Volume 306, Issue 5697, pp. 836-844 (2004)
[23] J. Kovac et al., Nature volume 420, pages 772–787(2002)
[24] Planck Collaboration, Planck 2018 results . IV, A&A 6 (2020)
[25] R. Genova-Santos et al, MNRAS, Volume 464, Issue 4, p.4107-4132 (2017)
[26] G. Puglisi, G. Fabbian and C. Baccigalupi, MNRAS, Volume 469, Issue 3, p.2982-2996 (2017)
[27] Planck Collaboration, Planck 2015 results. XXVI. A&A Volume 594, id.A26, (2016)
[28] G. Puglisi et al., ApJ, Volume 858, Issue 2, article id. 85, 14 pp. (2018).
[29] N. Krachmalnicoff et al., A&A Volume 618, id.A166, (2018)
[30] J.W. Henning et al., ApJ, Volume 852, Issue 2, article id. 97, 31 pp. (2018).
[31] T. Namikawa et al., The Simons Observatory Collaboration, arXiv:2110.09730 (2021).
[32] Th. Louis et al., Issue 06, article id. 031 (2017).
[33] BICEP2 Collaboration; Keck Array Collaboration, PRL, Volume 121, Issue 22, id.221301 (2018)
[34] S. Dahal et al., The CLASS Collaboration, arXiv:2107.08022
[35] L. Lamagna et al., Journal of Low Temperature Physics, (2020)
[36] The QUBIC Collaboration, Astroparticle Physics, Vol. 34, Issue 9, p. 705-716. (2011)
[37] The QUBIC Collaboration 2016, QUBIC Technical Design Report, arXiv:1609.04372
[38] The QUBIC Collaboration, Series of 8 QUBIC papers on JCAP special issue on QUBIC (2022)
[39] S. Masi et al., the QUBIC Collaboration, JCAP Special Issue (2022), arXiv:2008.10659
[40] G. D'Alessandro et al, The QUBIC Collaboration, JCAP Special Issue (2022), arXiv:2008.10667
[41] F. Cavaliere, et al., The QUBIC Collaboration, JCAP Special Issue (2022) arXiv:2008.12721
[42] C. O'Sullivan et al., The QUBIC Collaboration, JCAP Special Issue (2022), arXiv:2008.10119
[43] M. Piat, G. Stankowiak et al., The QUBIC Collaboration, JCAP Special Issue (2022), arXiv:2101.06787
[44] Charlassier, Bunn and Hamilton, A&A, Volume 514, id.A37 (2010)

[45] J.-Ch. Hamilton et al., A&A Volume 491, Issue 3, pp.923-927 (2008)
[46] S.A. Torchinsky, J.-Ch. Hamilton et al., The QUBIC Coll., JCAP Special Issue (2022), arXiv:2008.10056
[47] M.A. Bigot-Sazy and J.-Ch. Hamilton, A&A, Volume 550, id.A59 (2012)
[48] J.-Ch. Hamilton et al., The QUBIC Collaboration, JCAP Special Issue (2022), arXiv:2011.02213
[49] L. Mousset, M. Gamboa et al., The QUBIC Collaboration, JCAP Special Issue (2022), arXiv:2010.15119
[50] Review Board Report from Review organized by CNRS/IN2P3 with INFN participation (2020)
[51] D. Alonso et al., MNRAS, Volume 484, Issue 3, p.4127-4151 (2019)
[52] B. Thorne et al., MNRAS, Volume 469, Issue 3, p.2821-2833 (2017)
[53] Planck Collaboration, Planck Intermediate Results L., A&A, Volume 599, id.A51, 15 pp. (2016)
[54] A. Manzotti et al., SPTPol Collaboration, ApJ, Volume 846, Issue 1, article id. 45, 17 pp. (2017).
[55] S. Adachi et al., POLARBEAR Collaboration, PRL, Volume 124, Issue 13, article id.131301 (2020)
[56] J. Borrill, Proceedings of the 5th European SGI/Cray MPP Workshop", Bologna, Italy (1999)
[57] S. Vanneste et al., Phys. Rev. D 98, 103526 (2018)
[58] N. Perraudin et al., arXiv:1810.12186
[59] Planck Collaboration, Planck 2018 results. X. Constraints on inflation, submitted to A&A (2018)
[60] R. Gualtieri et al., SPIDER Collaboration, JLTP, Volume 193, Issue 5-6, pp. 1112-1121 (2018)
[61] M. Hazumi et al, LiteBIRD Collaboration, JLTP, Volume 194, Issue 5-6, pp. 443-452 (2019)
[62] J. Martin, Ch. Ringeval and V. Vennin, JCAP, Issue 10, article id. 038, (2014).
[63] J. Martin, Ch. Ringeval and V. Vennin, Physics of the Dark Universe, Volume 5, p. 75-235 (2014)
[64] R. Brandenberger and Z. Wang, Physical Review D, Volume 102, Issue 2, article id.023516 (2020)
[65] A. Ijjas and P.J. Steinhardt, Physics Letters B, Volume 795, p. 666-672 (2019)
[66] A. Roura, Albert, E. Verdaguer, Physical Review D, vol. 78, Issue 6, id. 064010 (2008)
[67] T. Markkanen et al., Physical Review D, Volume 91, Issue 8, id.084064 (2015)
[68] QUBIC-Argentina, Project Management Plan, internal QUBIC document (2021)
[69] Ade et al., BICEP/KECK Coll, arXiv:2110.00483
[70] M. Regnier et al., in preparation (2023) to be submitted shortly to A&A
[71] G. d'Alessandro et al., in preparation (2023)
[72] P. Chanial, M. Regnier, J.-Ch. Hamilton et al., in preparation (2023)
[73] M. Regnier et al., in preparation (2023)
[74] Abazajian, K., Addison, G. E., Adshead, P., et al. 2022, The Astrophysical Journal, 926, 54